ORIGINAL PAPER

Time-Resolved Fluorescence Anisotropy Study of the Interaction Between DNA and a Peptide Truncated from the p53 Protein Core Domain

Chengxuan Liu · Gaiting Liang · Zhen Liu · Lily Zu

Abstract Time-resolved fluorescence anisotropy spectroscopy was applied to study the interaction between a peptide truncated from the binding site of tumor suppressor p53 protein and the DNAs covalently labeled with 6-carboxyfluorescein (FAM) dye. Fluorescence intensity quenching and changes of anisotropy decay lifetime were monitored when FAM labeled DNA formed complex with the peptide. The results demonstrated that the sequence of DNA could not define the binding specificity between the peptide and DNA. But the anisotropy decay of FAM can be used to examine the binding affinity of the peptide to DNA. The fluorescent dynamics of FAM can also be used to represent the rigidity of the complex formed between the peptide and DNA.

Keywords Fluorescence spectroscopy · Time-resolved anisotropy · Interaction between peptide and DNA · Specific recognition

Introduction

Molecular recognition in protein-DNA interactions is central to many fundamental biological processes involved in regulating gene function. It had long been proposed that the sequence of the DNA acted as a template that selected the identity and coordinated the assembly of multiple proteins [1, 2]. However, recent studies of large amount of protein-DNA complexes suggested that the DNA sequence alone could not define the binding specificity between DNA and protein although there appeared to be favored interactions [3, 4].

C. Liu · G. Liang · Z. Liu · L. Zu (✉)
College of Chemistry, Beijing Normal University, Beijing 100875, Peoples Republic of China
e-mail: zull@bnu.edu.cn

Mutations occurred in the core domain of tumor suppressor p53 protein was identified relating to various human cancers [5–7]. Investigating the binding specificity of p53 to DNA is important to reveal the mechanism of its tumor suppressing process. In 1992, el-Deiry, et al. found out that the binding sequences within 18 human genomic clones that bound to p53 protein consisted of two copies of a 10 base pair motif 5′-PuPuPuC(A/T)(T/A)GPyPyPy-3′ separated by 0–13 base pairs (Pu and Py refers to purine and pyrimidine, respectively) [1]. Crystal structures and molecular dynamics simulation studies revealed that p53 core domain interacted with DNA mainly through hydrogen bonding of basic amino acid residues with DNA bases at the major groove and through van der Waal's contact at minor groove [2, 8–11]. The crystal structures showed the direct interactions between the p53 core domain and the target DNA but could not address the dynamics of the DNA recognition. NMR studies suggested that non-specific DNA also bound to p53 although not as tight as the specific DNA [12–14]. To understand the dynamics that define the binding specificity in solution, fluorescence approaches have been used to study the coupling between DNA and the p53 protein [15–24]. Weinberg et al. concluded that the p53 tetramer was required for increased binding affinity at high ionic strength by steady-state fluorescence anisotropy and analytical ultracentrifugation studies [16]. Ishimaru et al. suggested that binding of p53 to specific DNA resulted in a dramatic stabilization of the p53 protein compared to nonspecific sequence DNA [17]. While favored binding was supported in various experimental and theoretical studies, the role of the two decameric 'half-site' motifs in recognition of the p53 protein is still not fully understood.

In this work, the dynamics of the interaction between a peptide, RVCACPGRDRR (Arg-Val-Cys-Ala-Cys-Pro-Gly-Arg-Asp-Arg-Arg), truncated from the core domain of p53 protein (273–283) and a 20-mer DNA AGACATGCCTAGACATGCCT containing the two "half-site" decameric motifs are studied by time-dependent fluorescence anisotropy

spectroscopy. Unlike fluorescence intensity decay, anisotropy decay is very sensitive to the change of the dipole orientation [25–28]. Fluorescence anisotropy decay analysis can provide information of the rotational motion of the fluorophore and hence the properties of biological macromolecules which the fluorophore attaches. The truncated peptide contains the amino acid residues (Arg273, Ala276, Cys277, Arg280, Arg283) which interacting with the bases and the backbone of DNA at the major groove side [2, 9]. In order to focus the investigation on the interaction at the binding site and prevent the big size of p53 protein from reducing the sensitivity of the fluorescence measurements, the truncated peptide was used in this study. Fluorescence resonance energy transfer (FRET) method is also applied to study the interaction between the p53 truncated peptide and the target DNA. The binding specificity of the 20-mer DNA is compared with a 12-mer DNA TAGACA TGCCTT which containing only one "half-site" decameric motif. The result will help to understand the binding specificity of the p53 core domain to the DNA with the recognition unit, and evaluate the application of time-resolved fluorescence anisotropy measurements in studying the molecular recognition between protein and DNA.

Materials and Methods

Oligonucleotides and the peptide RVCACPGRDRR (HPLC purified) were provided by Shanghai Sangon Cooperative. The top strand oligonucleotides (5′-AGACATGCCTAGAC ATGCCT-3′ and 5′-TAGACATGCCTT-3′) were labeled with 6-carboxyfluoresein (FAM) at 5′-end via a six-carbon linker. For 12-mer DNA (5′-TAGACATGCCTT-3′ and 5′-TAGA TATTCCTT-3′), samples with FAM labeled on the base T^7 (the 7th base of the 12-mer DNA numbered from 5′-end) were also used for investigating the influence of the FAM location. To form a double-stranded DNA (dsDNA), the labeled oligonucleotide was hybridized with its unlabeled complementary strand in hybridization buffer (pH 7.2) prepared with 10 mM Tris (Aladdin, 100 %) and 10 mM NaCl (Beijing Chemical Works, 99.5 %). Oligomers were annealed by heating at the respective T_m for 10 min and then cooled to 25 °C over 20 min. The formation of the peptide-DNA complex was carried out at ambient temperature by adding peptide to the solution of dsDNA or single-stranded DNA (ssDNA) and mixed for 5 min. When FRET experiments were conducted, the acceptor fluorophore, 6-carboxytetramethylrhodamine (TAMRA) was covalently attached to the N-terminal of the peptide. The concentrations of DNAs used in the experiments were 5 μM. The concentration of the p53 truncated peptide was 5–150 μM, depending on the experiment. Millipore water (18.2 MΩ cm) was used throughout the experiments.

Steady-state spectroscopic experiments were carried out on TU-1901 UV Spectrometer (Persee, China) and Cary Eclipse

fluorescence spectrometer (Varian, American). Time-resolved fluorescence experiments were conducted on Tempro-01 spectrometer (IBH, UK) using the time-correlated single-photon-counting (TCSPC) technique. The excitation source was a pulsed laser diode (490 nm) with a repetition rate of 1 MHz and a pulse width <1.4 ns. Typically, 10000 photon counts were collected in the maximum 4096 channels. The decay parameters were determined by reconvolution analysis and the fitting quality was judged by the reduced χ^2 values and the randomness of the weighted residuals. Time-resolved anisotropy decay of FAM labeled on DNA was monitored. The anisotropy decay, $r(t)$, was derived according to the equation below [29],

$$r(t) = \frac{I_{VV}(t) - G \cdot I_{VH}(t)}{I_{VV}(t) + 2G \cdot I_{VH}(t)} \qquad (1)$$

in which the G factor was calculated by $G = I_{HV}(t)/I_{HH}(t)$, I represented the intensity of the fluorescence signal and the subscripts defined the orientation (H for horizontal and V for vertical) of the excitation and emission polarizers, respectively. In the exponential fitting of the anisotropy decay signal, the time when the signal of the prompt reached its maximum was selected as the time zero point because the prompt signal represented the instrumental response.

Results and Discussion

Steady-State and Time-Resolved Fluorescence Measurements

Absorption and fluorescence spectra of FAM 5′-end labeled 20-mer dsDNA and its complex with the peptide were first studied. A slight red shift (~2 nm) of the band peak in the
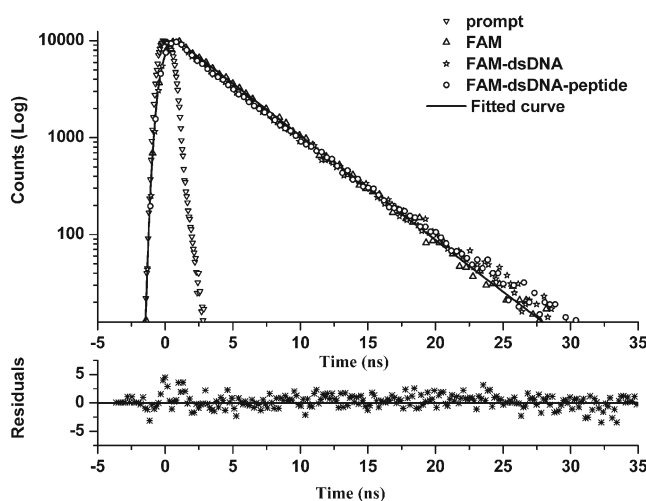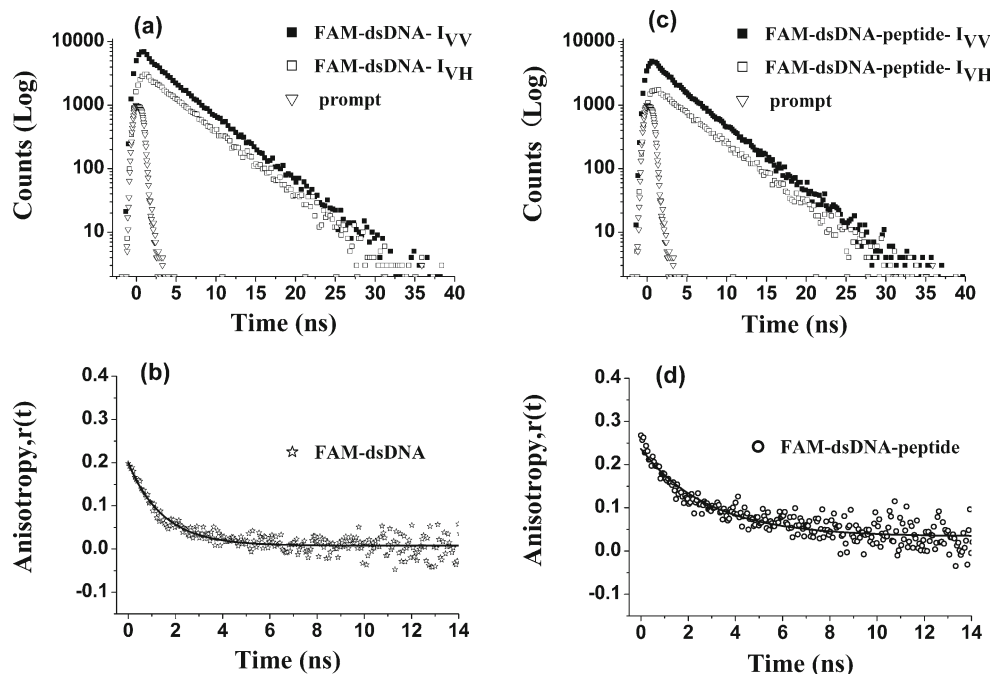

Fig. 1 Fluorescence intensity decay of free FAM in buffer, FAM-labeled 20-mer dsDNA (5 μM) and its complex formed with the peptide (DNA: peptide = 1:30)

Fig. 2 Measurements and the exponential fits of time-dependent anisotropy decay curves of 20-mer FAM-dsDNA (**a** and **b**) and FAM-dsDNA-peptide (**c** and **d**)

steady-state spectra was observed, but no lifetime difference was detected in the time-resolved fluorescence intensity decay curves when the dsDNA was in contact with the peptide (Fig. 1). When time-resolved fluorescence anisotropy signal was examined, significant difference was observed (Figs. 2 and 3). The anisotropy signal of free FAM in buffer solution exhibited single exponential decay decreasing from r_0 0.12 to r_∞ 0.00 with a short lifetime of 0.63 ns (Table 1), suggesting the fast rotation of free FAM in buffer solution. The r_0 value increased to 0.21 when FAM was attached to the 20-mer dsDNA. Exponential fits (Fig. 3) showed that the correlation time of the fluorescence anisotropy decay of FAM-dsDNA

increased to 1.46 ns. Increasing of the initial anisotropy r_0 and the depolarization time τ indicated that the orientation of FAM changed when it was covalently attached to dsDNA. Comparing to the rotational correlation time of free FAM, we assigned this longer decay time to the overall rotation diffusion of FAM-dsDNA. Rotational diffusion of fluorophores is a dominant cause of fluorescence depolarization, while the isotropic fluorescence data are insensitive to the orientation changes of electronic transition dipole moments [25, 30]. Changes of the decay time observed in the anisotropy depolarization experiments instead of in the fluorescence intensity decay measurements confirmed that the observed lifetime changes in the time-resolved fluorescence anisotropy spectra was due to the changing of the overall rotational diffusion rate of FAM in solution. The r_0 value further increased to 0.27 as the DNA-
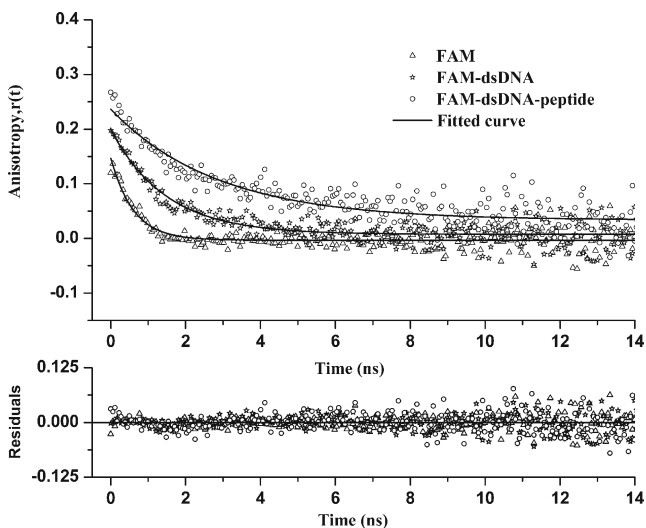
Fig. 3 Time-resolved fluorescence anisotropy decays of free FAM in buffer (△), 20-mer FAM-dsDNA (☆), and 20-mer FAM-dsDNA-peptide (○)

Table 1 Fluorescence anisotropy decay data for FAM in various environments

Sample	r_0	τ (ns)
free FAM	0.12	0.63
FAM-dsDNA(20-mer)	0.21	1.46
FAM-dsDNA(20-mer)-peptide	0.27	2.83
FAM-dsDNA(12-mer)	0.24	1.45
FAM-dsDNA(12-mer)-peptide	0.28	3.16
FAM^T-dsDNA(12-mer)	0.22	1.45
FAM^T-dsDNA(12-mer)-peptide	0.31	4.54
FAM^T-dsDNA(12-mer,TATT)	0.22	1.44
FAM^T-dsDNA(12-mer,TATT)-peptide	0.29	4.40

peptide complex formed. The depolarization lifetime also increased further to 2.83 ns, which was longer than the depolarization lifetime for the FAM-dsDNA. Thus reflected that the rotation of the FAM-dsDNA-peptide complex was slower than the FAM-dsDNA itself presumably due to the bigger size of the complex. To ensure whether there was a second component in the time-resolved anisotropy decay signals of the FAM-dsDNA and the FAM-dsDNA-peptide complex, biexponential fittings were tried [31]. No consistent lifetimes and corresponding amplitudes could be obtained if introducing a second component, i.e. no evidence for a biexponential anisotropy decay was observed. The experimental data suggested that the FAM-dsDNA and the FAM-dsDNA-peptide complex rotated as a rigid body without significant free rotation of the FAM group.

Time-resolved fluorescence anisotropy experiments of the 5′-end labeled 12-mer FAM-dsDNA (TAGACATGCCTT) with only one recognition unit and the complex it formed with the peptide were also conducted. No significant difference was observed compared to the results of 20-mer DNA (Fig. 4a). Therefore, under the condition of our experiments, no advanced binding specificity was detected for the full two "half-site" motifs compared to the 12-mer DNA containing only one "half-site" sequence. The anisotropy decay of a 12-mer FAM-dsDNA (TAGATATTCCTT), in which the C and G residues of the CATG center [1, 29] in the "half-site" motif was replaced by T bases, was also studied and no
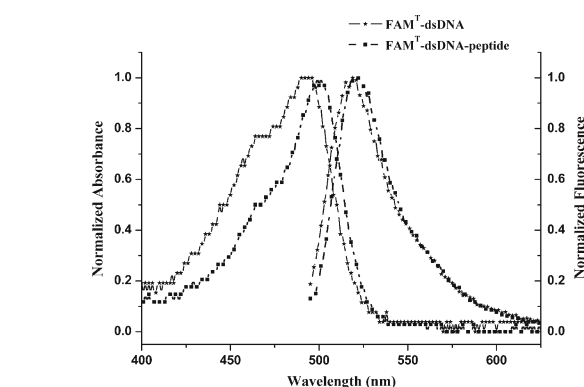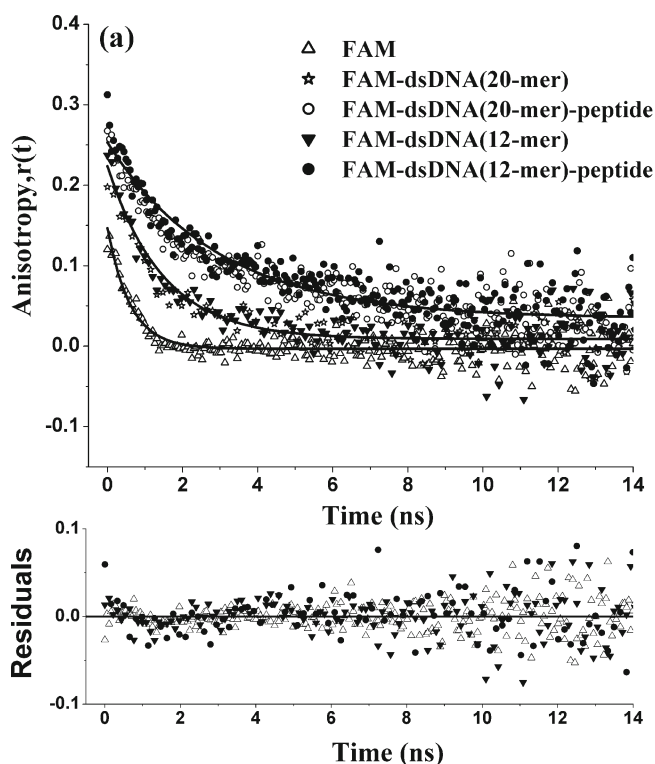

Fig. 5 Absorption and fluorescence spectra of 12-mer FAM^T-dsDNA (5 μM) and FAM^T-dsDNA-peptide (1:15), in which the superscript 'T' represents that FAM was labeled on the T^7 base of the DNA

significant difference was observed (Table 1). This result suggested that the dynamic role of the DNA sequence in defining the binding specificity between the peptide and the dsDNA was not significant. This might due to the nature of the interaction between proteins and DNA, which was the combination of hydrogen bonding, van der Waals forces, and electrostatic interactions instead of any one-to-one chemical bonding force [3, 32, 33]. The substitution of the central C and G bases in the DNA sequence eliminated the hydrogen bonding interaction between the two bases and the side chain of the basic residues of the peptide, but the quantitative effect might only become significant when large
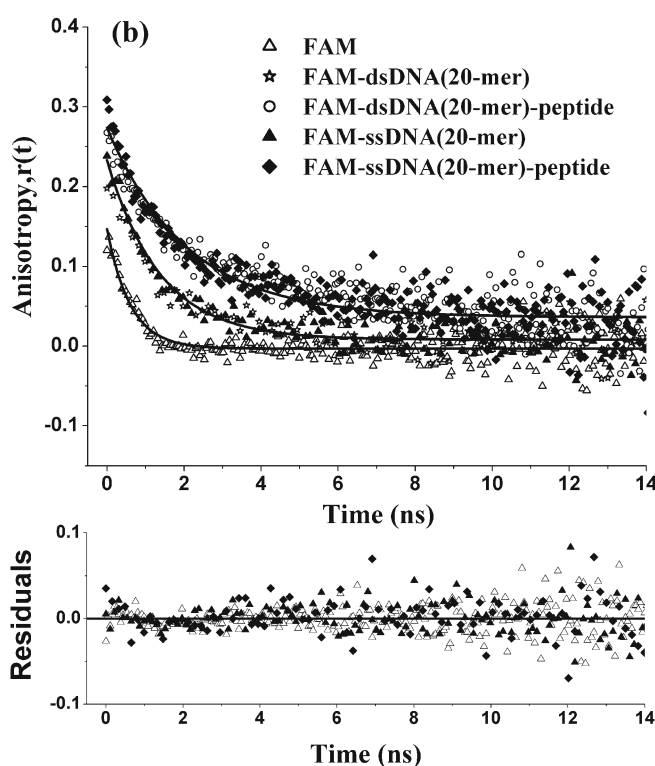

Fig. 4 The anisotropy decay curves of DNA-peptide complexes formed with 20-mer and 12-mer dsDNA (**a**) and the 20-mer ssDNA (**b**)

Fig. 8 Fluorescence quenching of 20-mer 5′-end labeled FAM-dsDNA by the TAMRA-peptide (dsDNA: peptide = 1:5)
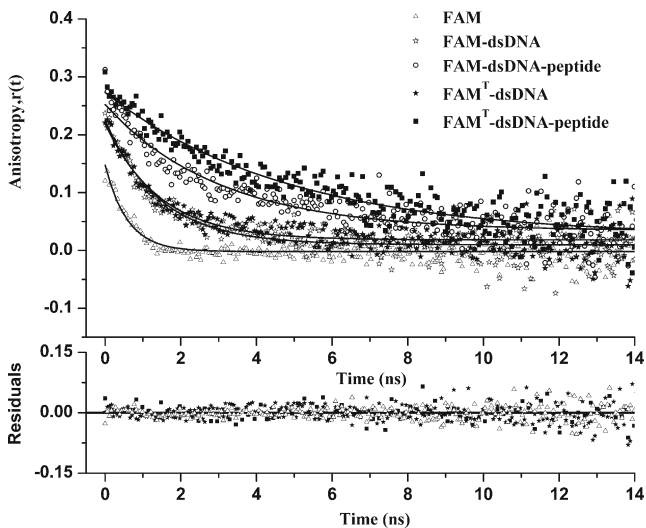
Fig. 6 Comparison of the time-dependent anisotropy decay curves of 12-mer T[7] labeled FAM[T]-dsDNA-peptide and 5′-end labeled FAM-dsDNA-peptide complexes

amount of hydrogen bonding interactions were affected in the formation of complex between the p53 protein and the DNA. The peptide RVCACPGRDRR truncated from the binding domain of p53 protein contained several basic amino acid residues. The basic residues could form hydrogen bonds and other interaction forces with different bases in the DNA sequence [3, 33], thus made the binding non-specific. Similar anisotropy decay curves obtained for the FAM-ssDNA and the FAM-ssDNA-peptide complex agreed with this assumption (Fig. 4b).

To exam the effect of the FAM location on DNA to the time-resolved fluorescence anisotropy study, the 12-mer DNA (TAGACATGCCTT) with FAM labeled on T[7], which was in the CATG center of the "half-site" motif specifically binding to the p53 protein [34], was used to repeat the experiments above. A distinct red shift (~7 nm) in the absorption spectrum was observed when the FAM[T]-dsDNA formed complex with the peptide (Fig. 5). A red shift of ~2 nm was also detected in the fluorescence spectrum. Compared to the negligible red
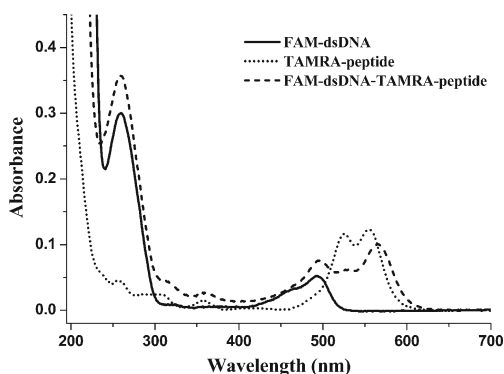

Fig. 7 Absorption spectrum of 20-mer FAM-dsDNA, TAMRA-peptide, and FAM-dsDNA-TAMRA-peptide (dsDNA: peptide = 1:5)
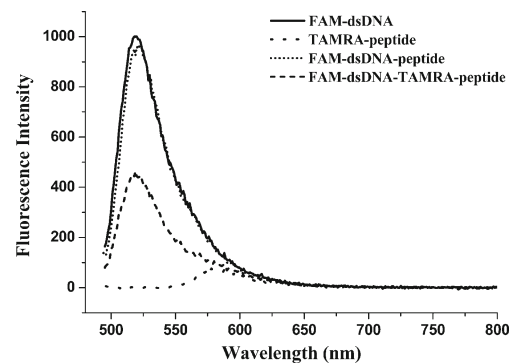
shift in the absorption spectrum of the 5′-end labeled FAM-dsDNA-peptide complex, it was obvious that the spectra of FAM were more sensitive to the interaction when it was labeled at a location close to the interaction site of the DNA-peptide complex. The time-resolved fluorescence anisotropy experiments supported this conclusion with a longer decay time recorded for the T[7] labeled FAM[T]-dsDNA-peptide complex (Fig. 6). However, labeling the fluorophore close to the binding site could not always be achieved practically when the binding site expanded over a long range of the DNA sequence or was unknown.

FRET Studies

When a second fluorophore TAMRA was labeled on the peptide, the interaction between the dsDNA and the peptide complex could be probed via the FRET effect between the donor FAM labeled on dsDNA and the acceptor TAMRA labeled on the peptide. In the absorption spectrum (Fig. 7) of the TAMRA-labeled peptide, the intensity of the blue band (525 nm) of TAMRA was strong due to the interaction between the labeled peptide molecules [35–38]. When the peptide formed complex with the dsDNA, the intensity of the 525 nm band decreased significantly and became a shoulder of the longer wavelength absorption band (~555 nm) of TAMRA. Similar phenomenon was reported by Spring et al. in the study of TAMRA labeled metal-DNA complex [36]. The experimental observation confirmed the formation of the dsDNA-peptide complex. Fluorescence quenching of the donor FAM induced by FRET effect was also observed but no significant increase of the acceptor fluorescence was recorded (Fig. 8). This might due to that the blue shoulder in the absorption spectrum of TAMRA corresponded to a dark state [36].

Conclusion

In this work, we studied the interaction between a peptide truncated from the binding domain of p53 protein and DNAs

with specific designed sequences by fluorescence spectroscopy of FAM labeled on DNA. The results revealed that the sequence of DNA could not define the binding specificity between the peptide and DNA. But the time-resolved fluorescence anisotropy spectroscopy can be used to examine the binding affinity of the peptide to DNA. The fluorescence anisotropy dynamics of FAM can also be used to represent the rigidity of the complex formed between the peptide and DNA. However, a detail mechanism of the binding specificity of the peptides to the duplex DNA remained unresolved for future research.

References

1. El-Deiry WS, Kern SE, Pietenpol JA, Kinzler KW, Vogelstein B (1992) Definition of a consensus binding site for p53. Nat Genet 1: 45–49

2. Cho Y, Gorina S, Jeffrey PD, Pavletich NP (1994) Crystal structure of a p53 tumor suppressor-DNA complex: understanding tumorigenic mutations. Science 265:346–355

3. Rhodes D, Schwabe JWR, Chapman L, Fairall L (1996) Towards an understanding of protein-DNA recognition. Phil Trans R Soc Lond B 351:501–509

4. Luscombe NM, Laskowski RA, Thornton JM (2001) Amino acid–base interactions: a three-dimensional analysis of protein-DNA interactions at an atomic level. Nucleic Acids Res 29:2860–2874

5. Badgwell DB, Walker CM, Baker WT, Strickland FM (2004) Ethanol and aloe emodin alter the p53 mutational spectrum in ultraviolet radiation–induced murine skin tumors. Mol Carcinogen 39:127–138

6. Rajesh M, Wang G, Jones R, Tretyakova N (2005) Stable isotope labeling-mass spectrometry analysis of methyl-and pyridyloxobutyl-guanine adducts of 4-(methylnitrosamino)-1-(3-pyridyl)-1-butanone in p53-derived DNA sequences. Biochemistry 44:2197–2207

7. Joerger AC, Fersht AR (2007) Structure-function-rescue: the diverse nature of common p53 cancer mutants. Oncogene 26:2226–2242

8. Nagaich AK, Zhurkin VB, Durell SR, Jernigan RL, Appella E, Harrington RE (1999) p53-induced DNA bending and twisting: p53 tetramer binds on the outer side of a DNA loop and increases DNA Twisting. Proc Natl Acad Sci U S A 96:1875–1880

9. Chen Y, Dey R, Chen L (2010) Crystal structure of the p53 core domain bound to a full consensus site as a self-assembled tetramer. Structure 18:246–256

10. Pan Y, Nussinov R (2008) p53-Induced DNA bending: the interplay between p53-DNA and p53-p53 interactions. J Phys Chem B 112: 6716–6724

11. Khavinson V, Shataeva L, Chernova A (2005) DNA double-helix binds regulatory peptides similarly to transcription factors. Neuroendocrinol Lett 26:237–241

12. Rippin TM, Freund SMV, Veprintsev DB (2002) Recognition of DNA by p53 core domain and location of intermolecular contacts of cooperative binding. J Mol Biol 319:351–358

13. Bell S, Klein C, Müller L, Hansen S, Buchner J (2002) p53 contains large unstructured regions in its native state. J Mol Biol 322:917–927

14. Joerger AC, Allen MD, Fersht AR (2004) Crystal structure of a superstable mutant of human p53 core domain. J Biol Chem 279: 1291–1296

15. Yang M, Ren LQ, Huang M, Kong RYC, Fong WF (1998) A DNA assay based on fluorescence resonance energy transfer and DNA triplex formation. Anal Biochem 259:272–274

16. Weinberg RL, Veprintsev DB, Fersht AR (2004) Cooperative binding of tetrameric p53 to DNA. J Mol Biol 341:1145–1159

17. Ishimaru D, Ano BoM AP, Lima LM, Quesado PA, Oyama MF, Gallo CV, Cordeiro Y, Silva JL (2009) Cognate DNA stabilizes the tumor suppressor p53 and prevents misfolding and aggregation. Biochemistry 48:6126–6135

18. Pavletich NP, Chambers KA, Pabo CO (1993) The DNA-binding domain of p53 contains the four conserved regions and the major mutation hot spots. Gene Dev 7:2556–2564

19. Bell S, Hansen S, Buchner J (2002) Refolding and structural characterization of the human p53 tumor suppressor protein. Biophys Chem 96:243–257

20. Bera A, Roche AC, Nandi PK (2007) Bending and unwinding of nucleic acid by prion protein. Biochemistry 46:1320–1328

21. Chen P-C, Hayashi MAF, Oliveira EB, Karpel RL (2012) DNA-interactive properties of crotamine, a cell-penetrating polypeptide and a potential drug carrier. PLoS ONE. doi:10.1371/jp0048913

22. Lan Y, Ye Y, Kozlowska J, Lam JKW, Drake AF, Mason AJ (2010) Structural contributions to the intracellular targeting strategies of antimicrobial peptides. Biochim Biophys Acta 1798:1934–1943

23. Khavinson VK, Solovyov AY, Shataeva LK (2006) Molecular mechanism of interaction between oligopeptides and double-stranded DNA. Bull Exp Biol Med 141:443–447

24. Delphin C, Cahen P, Lawrence JJ, Baudier J (1994) Characterization of baculovirus recombinant wild-type p53: dimerization of p53 is required for high-affinity DNA binding and cysteine oxidation inhibits p53 DNA binding. Eur J Biochem 223:683–692

25. Ma Y-Z, Shaw RW, Yu X, O'Neill HM, Hong K (2012) Excited-state dynamics of water-soluble polythiophene derivatives: temperature and side-chain length effects. J Phys Chem B 116:14451–14460

26. Shaw AK, Pal SK (2007) Fluorescence relaxation dynamics of acridine orange in nanosized micellar systems and DNA. J Phys Chem B 111:4189–4199

27. Yang J, Roller RS, Winnik MA (2006) Energy migration study of random immobile anthracene derivatives by time-resolved fluorescence anisotropy decays. J Phys Chem B 110:11739–11745

28. Zou M, Chen Y, Xu X, Huang H, Liu F, Li N (2012) The homogeneous fluorescence anisotropic sensing of salivary lysozyme using the 6-carboxyfluorescein-labeled DNA aptamer. Biosens Bioelectron 32:148–154

29. Lakowicz JR (2006) Principles of fluorescence spectroscopy. Springer, Berlin

30. Unruh JR, Gokulrangan G, Lushington GH, Johnson CK, Wilson GS (2005) Orientational dynamics and Dye-DNA interactions in a Dye-labeled DNA aptamer. Biophys J 88:3455–3465

31. Neuweiler H, Schulz A, Böhmer M, Enderlein J, Sauer M (2003) Measurement of submicrosecond intramolecular contact formation in peptides at the single-molecule level. J Am Chem Soc 125:5324–5330

32. Cai B-H, Chen J-Y, Lu M-H, Chang L-T, Lin H-C, Chang Y-M, Chao C-F (2009) Functional four-base A/T gap core sequence CATTAG of P53 response elements specifically bound tetrameric P53 differently than two-base A/T gap core sequence CATG bound both dimeric and tetrameric P53. Nucleic Acids Res 37:1984–1990

33. Sjakste N, Bielskiene K, Bagdoniene L, Labeikyte D, Gutcaits A, Vassetzky Y, Sjakste T (2012) Tightly bound to DNA proteins: possible universal substrates for intranuclear processes. Gene 492:54–64

34. Ho WC, Fitzgerald MX, Marmorstein R (2006) Structure of the p53 core domain dimer bound to DNA. J Biol Chem 281:20494–20502

35. Wang L, Gaigalas AK, Blasic J, Holden MJ, Gallagher DT, Pires R (2003) Fluorescence resonance energy transfer between donor-

acceptor pair on two oligonucleotides hybridized adjacently to DNA template. Biopolymers 72:401–412

36. Eckel R, Wilking SD, Becker A, Sewald N, Ros R, Anselmetti D (2005) Single-molecule experiments in synthetic biology: an approach to the affinity ranking of DNA-binding peptides. Angew Chem Int Ed 44:3921–3924

37. Chen T, Fu L, Zu L (2012) Steady-state and time-resolved fluorescence of tetramethylrhodamine attached to DNA: correlation with DNA sequences. Luminescence. doi:10.1002/bio.2446

38. Spring BQ, Clegg RM (2007) Fluorescence measurements of duplex DNA oligomers under conducive for forming M-DNA (a metal-DNA complex). J Phys Chem B 111:10040–10052